Structural Engineering and Mechanics, Vol. 8, No. 6 (1999) 561-578
DOI: http://dx.doi.org/10.12989/sem.1999.8.6.561

Time-dependent analysis of reinforced concrete structures using the layered finite element method

M.A. Bradford† and R.I. Gilbert†

School of Civil & Environmental Engineering, The University of New South Wales, Sydney, NSW 2052, Australia

S.C-H Sun‡

SMEC, North Sydney, NSW 2060, Australia

Abstract. The response of a reinforced concrete structure to loading is both immediate and time-dependent. Under a sustained load, the deflections caused by creep and shrinkage may be several times their instantaneous values. The paper describes a general finite element procedure, based on the so-called layered model, to analyse reinforced concrete members, and shows in particular how the simple Step by Step Method may be incorporated into this procedure. By invoking the Modified Newton Raphson Method as a solution procedure, the accuracy of the finite element method is verified against independent test results, and then applied to a variety of problems in order to demonstrate its efficacy. The method forms a general method for analysing highly indeterminate concrete structures in the time domain.

Key words: reinforced concrete; creep; finite elements; layered method; shrinkage; Step by Step Method; time effects.

1. Introduction

The response of a concrete structure subjected to service loading may be categorised into (i) short-term deformation and (ii) long-term deformation. The short-term behaviour is the instantaneous response of the structure under loading. This short-term relationship between the stress and strain follows the constitutive law that represents the material properties when the structure is considered over a short period of time. A number of researchers have considered only the idealised situation where the concrete is linearly elastic, but where the concrete has cracked in tension. In this situation, the short-term strain is usually called the elastic strain. If long-term effects are taken into account, the relationship between the total strains and stresses can no longer be considered as being described by a single constitutive law. This situation requires a nonlinear

† Professor
‡ Engineer

formulation in the time domain.

A very simple but important feature of this viscoelastic behaviour was introduced by Maslov (1940) and McHenry (1943), who stated that the strain (or stress) due to the sum of previous stress (or strain) histories is the sum of the individual responses. This statement implies that the principle of superposition is also applicable to aging concrete, which cannot be overlooked in the study of the long-term behaviour of concrete structures. As a result of this assumption, the so-called Step by Step procedure proposed by Ghali *et al.* (1969), Bazant and Najjar (1973), Schade (1977) and Neville *et al.* (1983) is used to predict the time-dependent behaviour as a result of the stress and strain history. Since the method is quite general and accurate in predicting the long-term strain for concrete members, it is the basic algorithm adopted for the time analysis described in this paper.

Apart from the Step-by-Step Method, other methods available to predict the time-dependent strain include the Effective Modulus Method (Faber 1927), the Age-Adjusted Effective Modulus Method (Trost 1967, Bazant 1972), the Rate of Creep Method (Glanville 1930, Whitney 1932, Dischinger 1937), the Rate of Flow Method (England and Illston 1965) and the Improved Dischinger Method (Nielsen 1970, Rusch *et al.* 1973). These methods are well-covered in the texts of Neville *et al.* (1983) and Gilbert (1988), and so no further attempt will be made to discuss them here as the present study is restricted to use of the Step-by-Step Method.

The 'cross-sectional analysis' technique assumes that the neutral axis of the stresses remains unchanged throughout the entire time domain, while restraining forces are calculated using the well-known relaxation procedure of Bresler and Selna (1964). This is not correct as the stress may change because of long-term effects. The cross-sectional analysis recognises this fact only when the restraining forces have been calculated. Therefore, the accuracy of calculating restraining forces using the cross-sectional method to predict the long-term behaviour is in doubt. Gilbert (1988) pointed out that a series of iterative numerical procedures are required to trace the movement of the neutral axis. More recently, Krishna Mohan Rao *et al.* (1993) used an iterative technique to update the 'creep-transformed' section in the time analysis, and this technique can obtain the correct location of the neutral axis.

For the nonlinear analysis of indeterminate concrete structures, the 'layered finite element analysis' (Bradford, Gilbert and Sun 1999) has been found to be more efficient than the so-called cross-sectional analysis. The basic criterion in the layered analysis is equilibrium. When equilibrium is established in the incremental and iterative process, the correct distribution of stresses and stains at Gaussian quadrature stations along a concrete member is available immediately. Therefore, in the layered finite element method, it is not necessary to re-calculate cross-sectional properties or to relocate the neutral axis for a cracked section.

Based on a formulation of stress and strain, the layered finite element method is capable of calculating the changes in strain and the changes in stress caused by long-term effects. The relaxation procedure proposed by Bresler and Selna (1964) is a powerful tool for the time analysis (as it is in the cross-sectional analysis), and is easily incorporated into the layered finite element method. Because the layered finite element method is stiffness-based, the long-term behaviour of concrete frames with many indeterminancies can be studied easily. Although Kang (1977) and Aldstedt and Bergan (1978) used the layered method for concrete frames, the way in which the stresses and strains were calculated were not alluded to in detail in their papers.

The most important feature of the layered finite element method is that the analysis of concrete structures under long-term loading can be simulated efficiently. The time-based analysis deploying the layered model can predict the long-term behaviour of multi-storey concrete frames. This paper

provides a comprehensive and systematic algorithm for the time-analysis of concrete frames, and when implemented in the layered finite element method developed by the authors (Bradford, Gilbert and Sun 1999) produces rapid and accurate solutions. These solutions are first verified against test results, and then illustrated by a series of examples.

2. The Step by Step Method (SSM) in finite element analysis

2.1. Material properties

The total strain ε, which depends on the time t, can be expressed as the sum of the instantaneous strain, creep strain and shrinkage strain as shown in Fig. 1 as follows:

$$\varepsilon(t) = \varepsilon_i(t_0) + \varepsilon_{cr}(t, t_0) + \varepsilon_{sh}(t) \tag{1}$$

where t_0 is the time at first loading. Under a sustained stress σ, the instantaneous or short-term strain $\varepsilon_i(t_0)=\sigma/E_c(t_0)$, where the modulus of elasticity is obtained from (ACI 1971)

$$E_c(t_0) = E_{c,28}\left(\frac{t_0}{A + Bt_0}\right)^{1/2} \tag{2}$$

in which A and B are coefficients which depend on the type of cement and curing conditions and $E_{c,28}$ is the tangential elastic modulus of the concrete 28 days after curing. When the stress is constant the creep strain is given by

$$\varepsilon_{cr}(t, t_0) = \phi(t, t_0)\, \varepsilon_i(t_0) \tag{3}$$

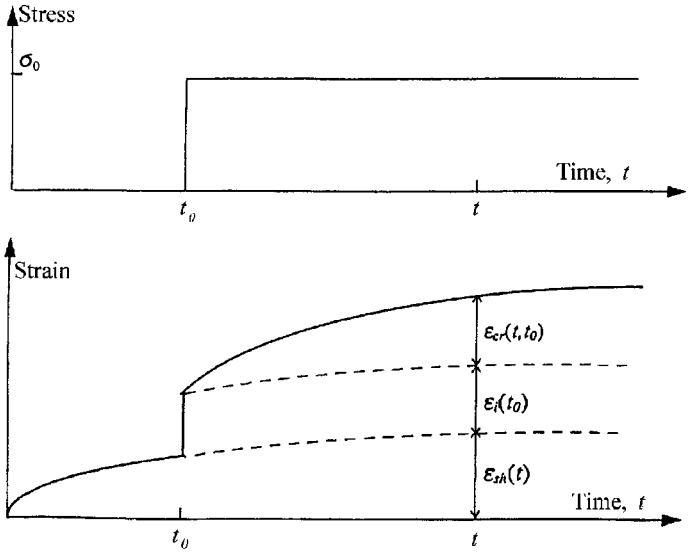

Fig. 1 Stress versus strain relationship in the time domain

where the creep coefficient ϕ is given empirically by the ACI (1971) as

$$\phi(t, t_0) = \frac{C(t - t_0)^F}{D + (t - t_0)^F} \tag{4}$$

which according to Branson *et al.* (1969) and Meyers *et al.* (1970) has the empirical form

$$\phi(t, t_0) = \frac{(t - t_0)^{0.6}}{10 + (t - t_0)^{0.6}} \phi_u(t_0) \tag{5}$$

where

$$\phi_u(t_0) = 125 t_0^{-0.118} \phi(\infty, 7) \tag{6}$$

Values of $\phi(\infty, t)$ are normally found in design codes. Eq. (6) introduces the concept of aging (Bazant 1972), where the aging effect decreases the final creep coefficient $\phi(\infty, t_0)$ as the time of first loading t_0 increases. This effect, presented by Distefano (1965) is shown in Fig. 2.

Finally, the shrinkage strain $\varepsilon_{sh}(t)$ is often expressed in terms of its long-term value ε^*_{sh} (Branson *et al.* 1969, Meyers *et al.* 1970) as

$$\varepsilon_{sh}(t) = \varepsilon^*_{sh} \frac{t}{d + t} \tag{7}$$

where d is 35 for moist curing and 55 for steam curing. Most current standards provide values of ε^*_{sh} for designers.

It should be noted that the empirical nature of Eqs. (2) and (4) to (7) has a marked influence on the numerical results, as these equations contain a number of parameters whose variation in predicting solutions by the numerical method developed herein can affect the final time-dependent response of the structure. The sensitivity of the calculated response of the structure to these experimentally-determined parameters is important, but is not considered explicitly in this paper as the focus is on the development of the numerical scheme.

2.2. Prediction of creep strain in the SSM

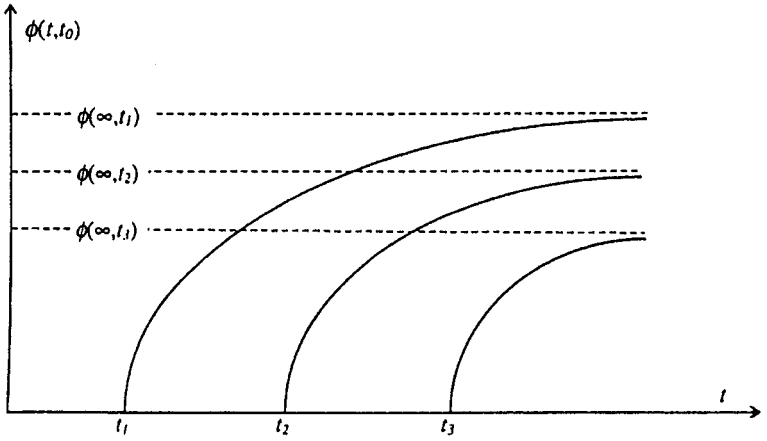

Fig. 2 Effect of age at first loading on the creep coefficient (after Distefano 1965)

Under constant loading, the long-term local stresses within a concrete structure change with time. These changes in local stresses may be thought of as being brought about by the internal indeterminacy of the concrete cross-section. Therefore, the change in stress should be considered when predicting the creep strain. The SSM is a convenient and efficient method that is used in this paper to predict creep strain due to time-varying stresses. Fig. 3 shows a typical relaxation time-dependent response of a concrete section subjected to an initial constant stress σ_0 (Neville *et al.* 1983).

The initial stress σ_0 is first applied at time t_0 and the stress normally reduces gradually due to the influence of creep strain. In order to account for the varying stress history, the time domain is subdivided into small segments. Bazant (1973) suggested that the selected times are best chosen in the form of a geometric progression, in which time steps are constant in the $\log(t - t_0)$ scale as given by

$$t_r = t_0 + (t_{r-1} - t_0) \cdot 10^s \tag{8}$$

Bazant also indicated a high accuracy is usually achieved with the first time step set to Δt_1=0.01 days and s in Eq. (8) normally ranges from 0.125 to 0.5. The larger the s value, the wider the time step. Although Bazant (1973) suggested that s be set equal to 0.5, it was found more convenient in this paper to set it equal to 0.3. It should be noted that care must be taken in the selection of s in the time analysis if the layered finite element method is used. The selection criteria is that the time step should not be too wide, in order to avoid the situation where no restraining forces are found when the relaxation procedure (Bresler and Selna 1964) is used. However, this situation was only found to occur if shrinkage strains are the major influence in the long-term response.

With t_0, Δt_1 and s given, Eq. (8) provides an automatic process to obtain the next time step from the current time. The creep strain at any particular time t_{r+1} is expressed by

$$\varepsilon_{cr}(t_0, t_{r+1}) = \frac{\sigma_0}{E(t_0)} \phi(t_{r+1}, t_0) + \sum_{j=1}^{r} \frac{\Delta\sigma(t_j)}{E(t_j)} \phi(t_{r+1}, t_j) \tag{9}$$

The first term on the right hand side of Eq. (9) is the creep strain due to the initial instantaneous strain. The summation on the right hand side of Eq. (9) accounts for the creep strain due to the changes in stress. This equation demonstrates that the SSM always uses the previous stress history to predict the current creep strain. It is assumed that the stress variation in each time step acts at the beginning of the next time step, as shown in Fig. 3.

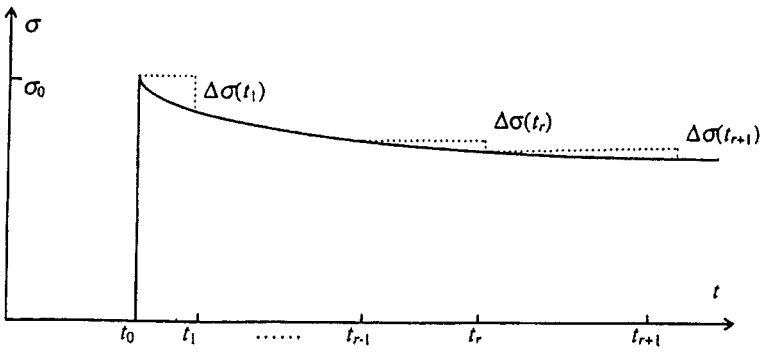

Fig. 3 Step-by-step method (after Neville *et al.* 1983)

Eq. (9) is suitable for a concrete section which does not crack. In the presence of cracking, it is more convenient to express Eq. (9) in terms of strains as

$$\varepsilon_{cr}(t_{r+1}) = \varepsilon_i(t_0)\phi(t_{r+1}, t_0) + \sum_{j=1}^{r} \Delta\varepsilon_i(t_j)\phi(t_{r+1}, t_j) \tag{10}$$

where $\varepsilon_i(t_0)$ and $\Delta\varepsilon_i(t_j)$ represent the initial instantaneous strain and the changes in instantaneous strain respectively. This formulation allows for material nonlinearity to be included, in particular cracking.

The SSM method has been criticised by Bazant (1973) because it is very difficult to store all the values of the stress (or strain) increments for all the previous time steps and to calculate the summations in Eqs. (9) and (10). A very crude estimate of about 100 time steps was advocated. In normal situations, there are about 25 time steps required to apply Eq. (9) when s is set equal to 0.4. If numerical difficulties are encountered, the solution is cut down to the preceding time step by reducing the s values. A similar method was used in the arc-length method of iterative analysis set out by the authors (Bradford, Gilbert and Sun 1999). The writers have encountered no numerical difficulties in the time analysis when s is set equal to 0.3.

With modern computer hardware, it is not difficult to store the stress (or strain) history for 25 time steps, although if out-of-core memory is used the computing speed is slowed a little to perform the summations in Eq. (10). However, the undoubted advantage of the SSM is that the change in position of the neutral axis in a cracked concrete section due to long-term effects is included in the time analysis. Another advantage of the SSM is that it is especially suitable for structures built or loaded in several stages, such as a precast segmental box girder bridge.

2.3. Incorporation into the finite element method

In the description of incorporating the time-dependent analysis into the finite element framework, the familiar mechanical strains will be defined as those strains which generate stresses, while non-mechanical strains refer to purely time-dependent strains that are not directly related to stress. Therefore, the total strains during a period of time are the sum of the mechanical and non-mechanical strains. In the treatment of viscoelastic problems, a nonlinear relationship will generally exist between the total strains and stresses, even if the instantaneous stress-strain relationship is assumed to be linear. Because of this, in the calculation of internal stresses, the non-mechanical strains must be separated from those mechanical strains which still have a linear relationship with the internal stresses during each time step.

The variations of stress and strain within a particular time step $t_{r+1} - t_r$, as shown in Fig. 3, is analysed herein by invoking the relaxation method (Gilbert 1988). The cross-sections are assumed to be frozen, so that the total strain is held initially constant. If the cross-sections are totally free of any restraint, then the non-mechanical strains at time t_{r+1} will include creep and shrinkage strains. The shrinkage strain can be computed from Eq. (7), giving

$$\varepsilon_{sh}(t_{r+1}, t_0) = \varepsilon_{sh}^* \frac{t_{r+1} - t_0}{d + (t_{r+1} - t_0)} \tag{11}$$

The creep strain at the end of this time step is computed from Eq. (10), provided the previous stress (or strain) history is known. The creep coefficient $\phi(t_{r+1}, t_j)$ in Eq. (10) is given by Eq. (5), with the time interval set equal to $t_{r+1} - t_j$. Obviously the effect of aging on concrete creep is

included by using the SSM. The total non-mechanical strain at the end of the current time step is equal to

$$\varepsilon_{nm}(t_{r+1}) = \varepsilon_{cr}(t_{r+1}, t_0) + \varepsilon_{sh}(t_{r+1}, t_0) \tag{12}$$

noting that t_0 is the time at which the loading is first applied. If there are other loads applied at time $t_k < t_{r+1}$, the creep strain at time t_{r+1} is

$$\varepsilon_{cr}(t_{r+1}) = \sum_k \left(\varepsilon_i(t_{k-1})\, \phi(t_{r+1}, t_{k-1}) + \sum_{j=k-1}^{r} \Delta\varepsilon_i(t_j)\, \phi(t_{r+1}, t_j) \right) \tag{13}$$

Eq. (13) is only valid if the principle of superposition is applied.

The incremental non-mechanical strains $\Delta\varepsilon_{nm}(t_r)$ at time t_{r+1} are clearly obtained from

$$\Delta\varepsilon_{nm}(t_r) = \varepsilon_{nm}(t_{r+1}) - \varepsilon_{nm}(t_r) \tag{14}$$

The non-mechanical strains at each time step must be stored. Since the structure is still frozen at this stage, an equal and opposite incremental non-mechanical strain $-\Delta\varepsilon_{nm}(t_r)$ must be applied to the concrete only to restore compatibility. The current mechanical strain $\varepsilon_m(t_{r+1})$ is given by

$$\varepsilon_m(t_{r+1}) = \varepsilon_m(t_r) - \Delta\varepsilon_{nm}(t_r) \tag{15}$$

With the current mechanical strain $\varepsilon_m(t_{r+1})$, the current state of stress $\sigma(t_{r+1})$ is calculated according to the constitutive law as

$$\sigma(t_{r+1}) = \sigma(\varepsilon_m(t_{r+1})) \tag{16}$$

which can simply be written for the constitutive law adopted here as

$$\sigma(t_{r+1}) = E(t_{r+1})\varepsilon_m(t_{r+1}) \tag{17}$$

By integrating the current state of stress $\sigma(t_{r+1})$ throughout the entire element, the current internal force vector $\{F(t_{r+1})\}$ for use in the finite element formulation is given by

$$\{F(t_{r+1})\} = \int_V <B>^T \sigma(t_{r+1})\, dV \tag{18}$$

where V is the volume of the element, and $<B>$ is a strain matrix that may include geometric nonlinearity (Bradford, Gilbert and Sun 1999). The out-of-balance load vector $\{P_u(t_{r+1})\}$ is calculated by subtracting the current internal force vector from the current external loading vector $\{P(t_{r+1})\}$, and this gives

$$\{P_u(t_{r+1})\} = \{F(t_{r+1})\} - \{P(t_{r+1})\} \tag{19}$$

Since the long-term effects are now being considered, the current external service load vector $\{P_u(t_{r+1})\}$ varies with time. Using the principle of superposition, the structure is released and equilibrium is restored by applying the current unbalanced load vector $\{P_u(t_{r+1})\}$ to the structure. From this point, the standard Modified Newton Raphson method can be used, and the current incremental displacement vector $\{\Delta r(t_r)\}$ caused by $\{P_u(t_{r+1})\}$ is

$$\{\Delta r(t_r)\} = [\bar{\bar{K}}]_T^{-1}\{P_u(t_{r+1})\} \tag{20}$$

where $[\bar{\bar{K}}]_T$ is the time-varying structural tangent stiffness matrix given by Bradford, Gilbert and

Sun (1999). It is important to recognise that the stresses and strains created after the structure is released are mechanical. With this current incremental displacement $\{\Delta r(t_r)\}$, the current incremental strain after the structure is released is

$$\Delta\varepsilon_m(t_r) = <B>\{\Delta r(t_r)\} \tag{21}$$

Using Eq. (15), the current mechanical strain, updated from the previous mechanical strain and the incremental strain after the structure is released is

$$\varepsilon_m(t_{r+1}) = \varepsilon_m(t_r) - \Delta\varepsilon_{nm}(t_t) + \Delta\varepsilon_m(t_r) \tag{22}$$

The constitutive relationship allows the current state of stress to be expressed in terms on the current mechanical strain, and is calculated from Eq. (16). The current displacement vector $\{r(t_{r+1})\}$ is also updated using the previous displacement vector $\{r(t_r)\}$ and the incremental displacement after the structure is released. The current displacement vector is therefore

$$\{r(t_{r+1})\} = \{r(t_r)\} + \{\Delta r(t_r)\} \tag{23}$$

3. Experimental verification

3.1. Goyal and Jackson's Columns

Goyal and Jackson (1971) performed a comprehensive experimental investigation into the behaviour of reinforced concrete columns under sustained loads. The columns were of uniform square cross-section with 76 mm sides, and reinforced symmetrically with four bars with a cover of 13 mm. Other details of the tests can be found in Goyal and Jackson's paper.

Columns 'G', 'H' and 'R' (Goyal and Jackson 1971) were subjected to differing sustained loads at differing eccentricities and also different areas of reinforcement. The rheological modelling of the concrete in the time domain was based on the material model presented in this paper as well as the SSM, and assumed that the final creep coefficient and shrinkage strains were 2.0 and -200×10^{-6} respectively. The comparison in Fig. 4 between the experimental results and those determined by the finite element model are very good, particularly so for Column 'R' whose time-dependent behaviour is markedly nonlinear.

3.2. Furlong and Ferguson's Frames

The major advantage of the numerical technique is in the modelling of frame structures. Furlong and Ferguson (1966) tested rectangular frames of the type shown in Fig. 5. Details of the geometry and material properties can be found in Furlong and Ferguson's paper. Frame '7' is of particular interest, as it was loaded to about 60% of its calculated ultimate strength, and this load was maintained for 102 days, and the frame then loaded to failure.

Fig. 6 shows the finite element and layer modelling for the frames. Frame '7' was analysed by the numerical model described herein, and the comparison of test and theory is shown in Fig. 7. A final creep coefficient of 2.0 but no shrinkage strain (Furlong and Ferguson 1966) was used in the modelling of the sustained portion of the loading regime. The figure shows that the agreement between test and theory is very good, both for the short-term response and for the time-dependent deflections when the load was held constant for 102 days. The accuracy of the finite element strength model (Bradford, Gilbert and Sun 1999), which is used as the shell for the time-

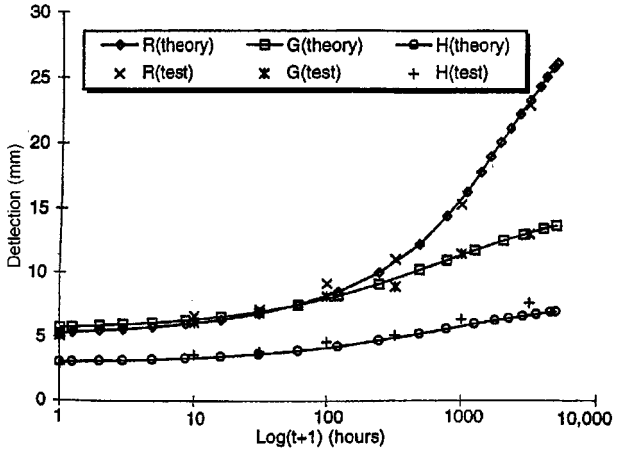

Fig. 4 Deflection-time curves for Goyal's columns G, H and R

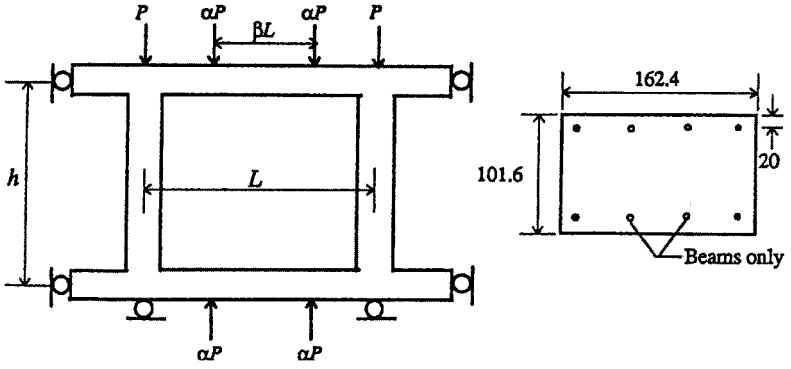

Fig. 5 Furlong and Ferguson's frame tests

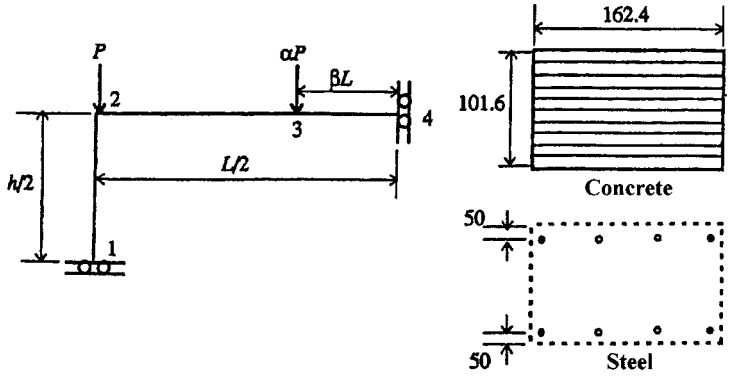

Fig. 6 Finite element and layer modelling of Furlong and Furguson's frames

dependent analysis developed in this paper, is also evident in Fig. 7 at loads above that which was sustained where both short-term material and geometric nonlinearities are dominant.

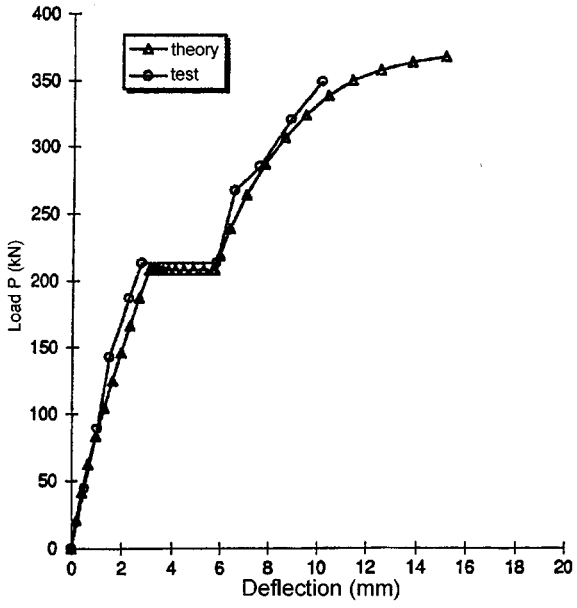

Fig. 7 Load-deflection response of Furlong and Furguson's 'Frame 7' with a sustained load

The close agreement between the SSM finite element-based method (with its empirical treatment of the 'material' aspects of creep and shrinkage) and the isolated column and frame tests demonstrates that the numerical model can be used with confidence to analyse a myriad of reinforced concrete members and frames subjected to creep and shrinkage.

4. Illustrative examples

4.1. General

In order to illustrate the efficacy of the layered finite element method using the SSM, a number of illustrative examples were chosen. These are for an isolated cross-section, a statically determinate beam, a statically indeterminate beam, and finally a frame structure. The problems were solved on a contemporary personal computer, and the solution of the Modified Newton Raphson iterative procedure was rapid.

4.2. Reinforced concrete cross-section

The long-term behaviour of a reinforced concrete cross-section was considered using the layered finite element model, and compared with the solutions derived using the so-called cross-sectional method (Sun 1996). The cross-section is shown in Fig. 8, which is subjected to an in-service bending moment of 60 kNm. The final creep coefficient was assumed to be $\phi^*=2.5$ and the long-term shrinkage strain was assumed to be $\varepsilon^*_{sh}=-400\times10^{-6}$. In the numerical analysis reported herein, the cross-section was divided into 20 equal concrete layers and the steel

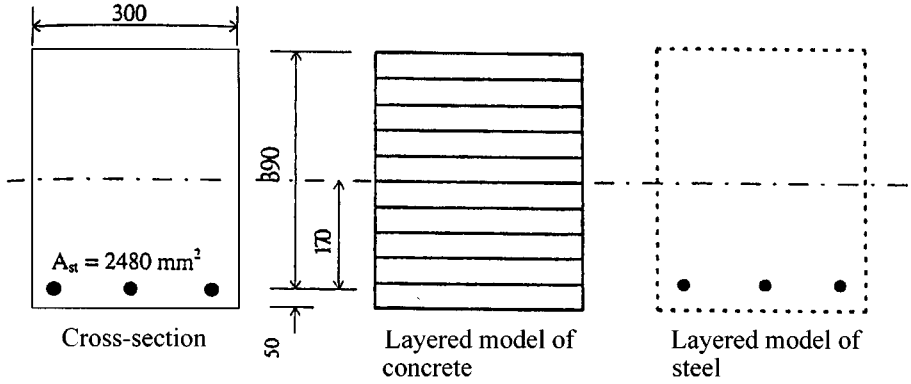

Fig. 8 Reinforced concrete cross-section

reinforcement into one layer.

The initial and final stress and strain distributions predicted by the two methods are shown in Fig. 9. The values in brackets are the long-term tensile stresses in the steel. It can be seen that the short-term stresses and strains are very close if the values at the midheight of layer 1 and layer 20 are extrapolated to the extreme fibres of the section. Fig. 9(a) shows that the Age-Adjusted

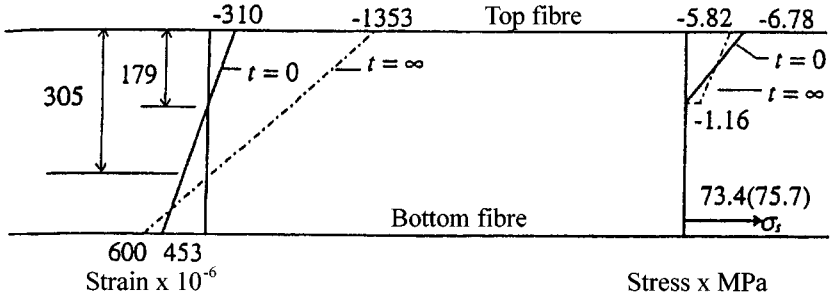

(a) Analysis using the cross-sectional method combined with the AEMM

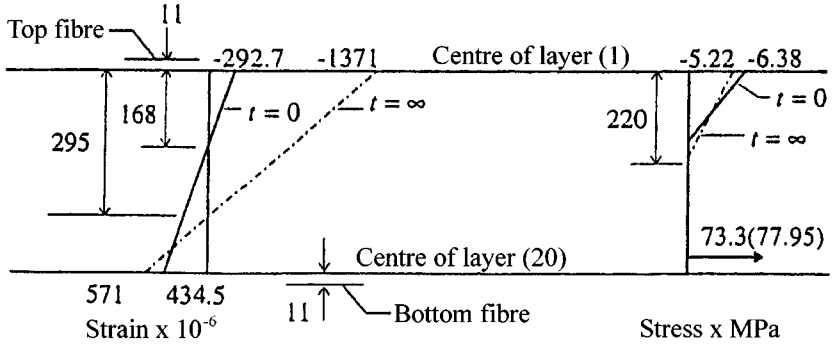

(b) Analysis using the layered finite element model

Fig. 9 Time analysis of a reinforced concrete section

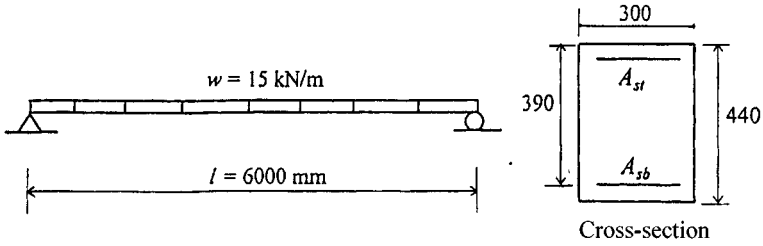

Fig. 10 Simply supported beam

Effective Modulus Method approach uses the same location of the neutral axis of the section in the short and long-term. The short-term neutral axis depth obtained from the cross-sectional method was 179 mm from the top fibre, but that extrapolated from the SSM was 231 mm. This difference leads to different internal stress and strain distributions in both the concrete and reinforcement. If the correct location of the neutral axis is required from the cross-sectional method, an iterative procedure must be undertaken.

4.3. Statically determinate beam

Since long-term effects increase the internal strains in concrete sections significantly, they also increase the deformations of concrete members. As an example, a simply supported reinforced concrete beam spanning 6 m shown in Fig. 10 was analysed. This beam was analysed in Warner *et al.* (1989). The singly reinforced beam was divided into ten layers of equal thickness, with a single layer adopted for the steel 170 mm from the reference line. The constitutive stress-strain curve was adopted from Bradford, Gilbert and Sun (1999), with a concrete compressive strength of 24 MPa, a concrete tensile strength of 1.2 MPa, a steel yield stress of 400 MPa and an initial elastic modulus of the concrete of 21,800 MPa. The long-term behaviour of this beam was investigated by varying the arrangement of both the tensile and compressive reinforcement.

The beam was subjected to a uniformly distributed sustained load of w=15 kN/m, with the final creep coefficient and shrinkage strain being 2.5 and -300×10^{-6} respectively.

The short-term and long-term central deflections of the beam were calculated using the layered approach coupled with the SSM, and the results are presented in Tables 1 and 2. In Table 1, the tensile reinforcement was kept constant and the compressive reinforcement varied, while the opposite situation occurred in Table 2. It can be seen from both tables that the short-term and long-term deformations decrease significantly as the amount of reinforcement increases. As expected, though, increasing the quantity of tensile reinforcement has less of an effect on the reducing the long-term deflections.

Table 1 Long-term behaviour of determinate beam with A_{sb}=2480 mm^2

Central Deflection (mm)	A_{st}=0	A_{st}=0.5A_{sb}	A_{st}=A_{sb}	A_{st}=2A_{sb}
Short-term (1)	9.74	7.65	6.50	5.63
Long-term (2)	27.07	12.58	9.17	6.92
(2) - (1)	17.33	4.93	2.67	1.29

Table 2 Long-term behaviour of determinate beam with A_{st}=1240 mm^2

Central Deflection (mm)	A_{sb}=0.5A_{st}	A_{sb}=A_{st}	A_{sb}=1.5A_{st}	A_{sb}=2A_{st}
Short-term (1)	20.74	12.14	9.27	7.95
Long-term (2)	25.68	16.99	14.09	12.58
(2) - (1)	4.94	4.85	4.82	4.93

4.4. Statically indeterminate beam

Long-term effects do not change the internal forces in a statically determinate member, such as the beam considered above, but they do change the internal forces of a statically indeterminate member. To demonstrate this, the propped cantilever shown in Fig. 11 was analysed. The material properties were the same as those considered in the analysis of a plain cross-section, with half of the beam reinforced by both top and bottom reinforcement each of area 2480 mm^2, and the other half of the beam reinforced by a single layer of reinforcement of area 2480 mm^2. The beam was discretised into eight equal length elements, each containing three Gauss points. The concrete section was further subdivided into 10 layers of equal thickness.

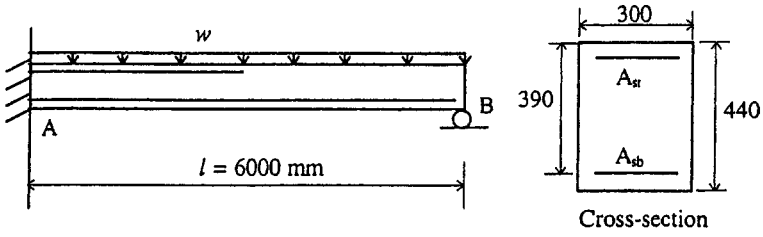

Fig. 11 Propped cantilever

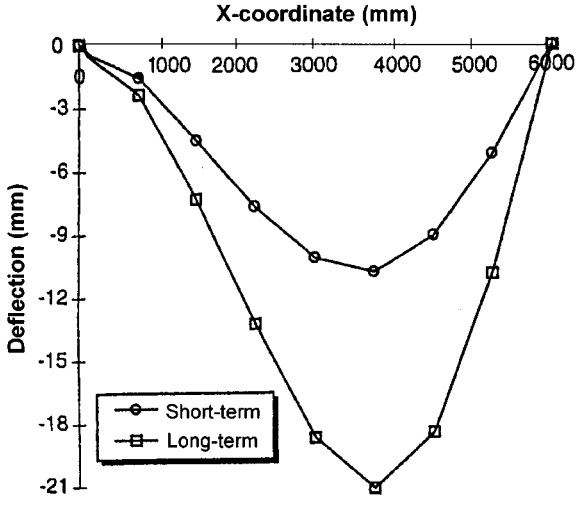

Fig. 12 Short and long-term deflections of propped cantilever

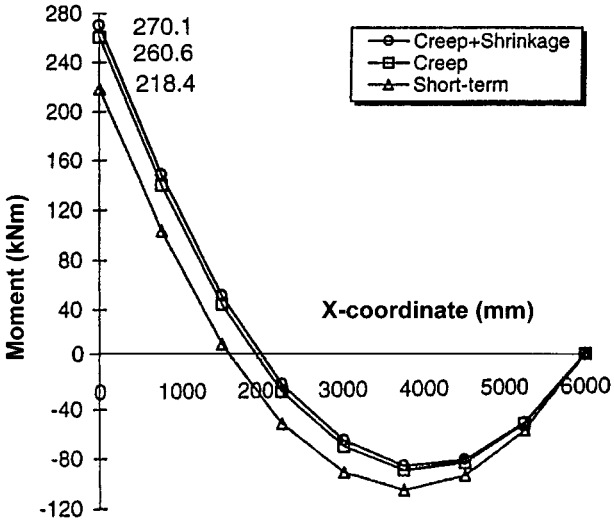

Fig. 13 Short and long-term bending moments in propped cantilever

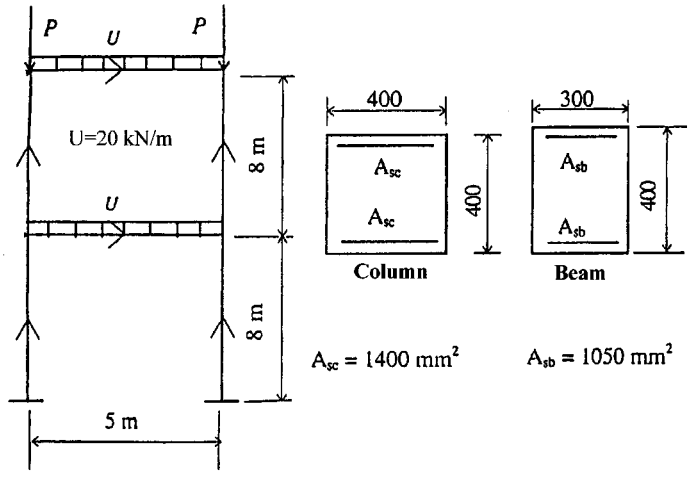

Fig. 14 Two-storey reinforced concrete frame

The computed deflections are shown in Fig. 12. It can be seen from this figure that the deflections are roughly doubled in the long-term.

In a statically indeterminate member, releasing the redundancy violates geometric compatibility, in the sense that the incompatibility of deflections at the release point increases with time. In order to restore compatibility, a time-varying redundant action must be applied at the release point. Fig. 13 plots the bending moment diagram and shows that in the time domain the positive moments are reduced, while the negative moments at the cantilever root are increased. If the end B of the member shown in Fig. 11 was released, the effects of creep and particularly shrinkage would cause this 'free' end to move upward as there is more tensile than compressive reinforcement in this region. Equilibrium must therefore be ensured by application of a downward reaction, and this time-dependent secondary force produces a secondary moment that is 24% of the original moment at the fixed end. A similar problem was analysed by Gilbert (1988) using the

flexibility method of structural analysis coupled with the Age-Adjusted Effective Modulus Method.

4.5. Reinforced concrete frame

The demonstrations of the application of the present SSM in a layered finite element shell have only been for simple structures. The power of this method is that it can handle structures with many indeterminancies, such as reinforced concrete frames. The writers have found very few published results on the long-term analysis and behaviour of highly indeterminate frames, so the present method was used to analyse a two storey reinforced concrete frame shown in Fig. 14. The material properties for the steel and concrete are the same as those considered earlier for the simple cross-section, with $\phi^*=2.5$ and $\varepsilon^*_{sh}=-300\times10^{-6}$. Five elements were used for each

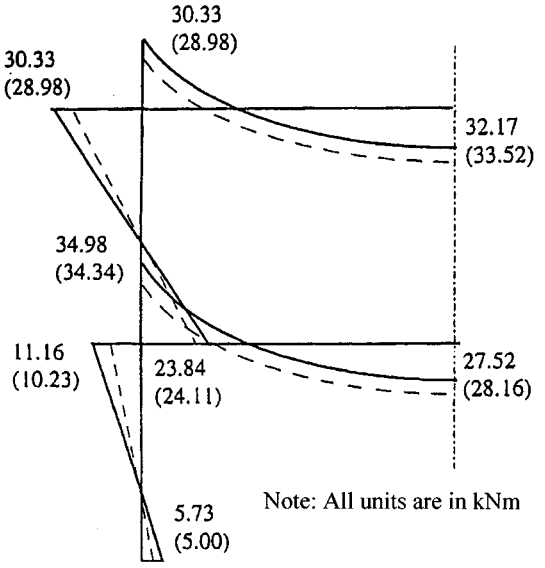

Fig. 15 Short and long-term bending moments in two-storey frame

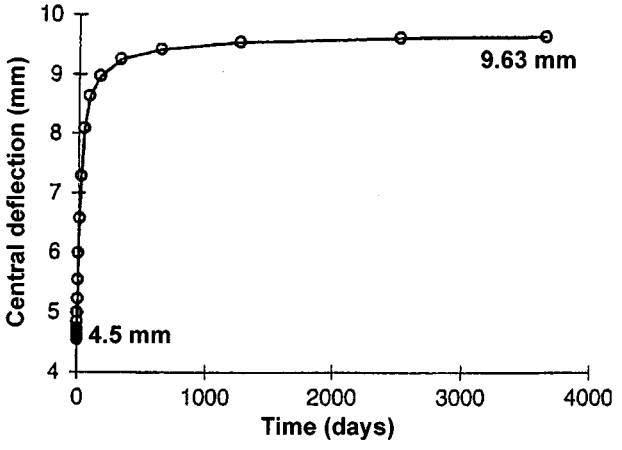

Fig. 16 Central deflection of beam at first floor level in two-storey frame

member.

The short-term and long-term bending moment diagrams for this frame are shown in Fig. 15. Horizontal loading was not considered, as this would be due to wind (or earthquake) loading and is not sustained for a long-term analysis. The moments are drawn on the tension side of the members, with those given in brackets being the long-term moments. It can be seen that the moment redistribution is quite substantial, with part of the end moments of the beam being redistributed to their mid-section. It is also worth noting that compared with the propped cantilever considered earlier, the long-term effects on the internal actions in this symmetric concrete frame are small.

The central deflection of the midspan of the beam at the first floor level is shown in Fig. 16 over a period of ten years. The final long-term deflection is more than twice its short-term deflection, but since the whole beam moves vertically by 3.383 mm due to shortening of the columns, the net long-term relative deflection is 6.247 mm or about span/800. This deflection would be deemed to be satisfactory.

5. Conclusions

A method for including the SSM of time-dependent analysis into a finite element computer package has been described. This algorithm was especially designed for the nonlinear finite element procedure developed by the authors (Bradford, Gilbert and Sun 1999). The solutions converge rapidly using the Modified Newton Raphson Method, and recourse is not required to more complex arc-length procedures that are necessary to trace the full load-deflection history for the strength limit state.

The accuracy of the method was established by comparisons with independent test results, and its efficacy was demonstrated by considering a simple cross-section, a determinate beam, an indeterminate beam and finally a two storey frame. The solutions were obtained with ease from the numerical method. The numerical approach developed in the paper provides a useful means of evaluating the provisions of the simplified methods presented in code rules.

While the numerical modelling is based on accurate principles of structural mechanics, the precision with which the creep and shrinkage data can be specified must not be lost sight of. The empirical nature of these parameters undoubtedly affects the final solution, and the finite element modelling is an ideal means for assessing the sensitivity of the final results to the empirical time-dependent data. This aspect of the material modelling has not been considered explicitly in this paper.

References

ACI Committee 209 (1971), "Prediction of creep, shrinkage and temperature effects in concrete structures", *Designing for the Effects of Creep, Shrinkage, and Temperature in Concrete Structures*, SP-27, *ACI*, 51-93.

Aldstedt, E. and Bergan, P.G. (1978), "Nonlinear time-dependent concrete frame analysis", *Journal of the Structural Division, ASCE,* **104**(ST7), 1077-1092.

Bazant, Z.P. (1972), "Prediction of concrete creep effects using age-adjusted effective modulus method", *ACI J.,* **69**, 212-217.

Bazant, Z.P. (1973), "Theory of creep and shrinkage in concrete structures: A precis of recent

developments", *Mechanics Today,* **2**, Pergamon Press, Oxford.
Bazant, Z.P. and Najjar, L.J. (1973), "Comparison of approximate linear models for concrete creep", *Journal of the Structural Division, ASCE,* **99**(ST9), 1851-1874.
Bradford, M.A., Gilbert, R.I. and Sun, S.C-H. (1999), "Advanced strength analysis of R-C frames using a layered FEM", submitted for publication.
Branson, D.E., Meyers, B.L. and Kripanarayanan, K.M. (1969), "Time-dependent deformation of non-composite and composite sand-lightweight prestressed concrete structures", Iowa Highway Commission Research Report, No. 69-1, University of Iowa, Iowa City.
Bresler, B. and Selna, L. (1964), "Analysis of time dependent behaviour of reinforced concrete structures", *Symposium on Creep of Reinforced Concrete Structures, ACI J. SP-9,* **55**, 321-345.
Dischinger, F. (1937), "Untersuchungen uber die Knicksicherheit, die elastische Verformung und das Kriechen des Betons bei Bogenbrucken", *Der Bouingenieur,* **18l**, No. 33/34, 487-520; No. 35/36, 539-552; No. 39/40, 595-621.
Distefano, J.N. (1965), "Creep buckling of slender columns", *Journal of the Structural Division, ASCE,* **91**(ST3), 127-150.
England, G.L. and Illston, J.M. (1965), "Methods of computing stress in concrete from a history of measured strain", *Civil Engineering and Public Works Review,* **60**, No. 705, 513-517; No. 706, 692-694; No. 707, 846-847.
Faber, O. (1927), "Plastic yield, shrinkage and other problems of concrete and their effect on design", *Minutes of Proceedings of Institution of Civil Engineers,* **225**, Part I, London, 27-73.
Furlong, R.W. and Ferguson, P.M. (1966), "Tests on frames with columns in single curvature", *Symposium on Reinforced Concrete Columns*, ACI SP-13, 55-73.
Ghali, A., Neville, A.M. and Jha, P.C. (1967), "Effect of elastic creep recoveries of concrete on loss of prestress", *ACI J.,* **64**, 8-2-810.
Gilbert, R.I. (1988), *Time Effects in Concrete Structures*, Elsevier, Amsterdam.
Glanville, W.H. (1930), "Studies in reinforced concrete III: The creep or flow of concrete under load", *Building Research Technical Paper* No. 12, Department of Scientific and Technical Research, London.
Goyal, B.B. and Jackson, N. (1971), "Slender concrete columns under sustained load", *Journal of the Structural Division, ASCE,* **97**(ST11), 2729-2750.
Kang, Y.J. (1977), "Nonlinear geometric, material and time-dependent analysis of reinforced and prestressed concrete frames", Thesis presented to the University of Southern California at Berkley, Ca., in partial fulfilment of the requirements for the degree of Doctor of Philosophy.
Krishna Mohan Rao, S.V., Prasada Rao, A.S. and Dilger, W.H. (1993), "Time-dependent analysis of cracked partially prestressed concrete members", *Journal of Structural Engineering, ASCE,* **119**(12), 3571-3589.
Maslov, G.N. (1940), "Thermal stress state in concrete masses with account to creep of concrete", Izvestia Nauchno-Issledovatelskogl Instituta VNII, Gidrotekhniki, Gosenergoizdat, USSR, **28**, 175-188.
McHenry, D. (1943), "A new aspect of creep in concrete and its application to design", *Proceedings, ASTM,* **43**, 1069-1086.
Meyers, B.L., Branson, O.E., Schumann, C.G. and Christiason, M.L. (1970), "The prediction of creep and shrinkage properties of concrete", Highway Commission Report No. HR-136, University of Iowa, Iowa City.
Neville, A.M., Dilger, W.H. and Brooks, J.J. (1983), *Creep of Plain and Structural Concrete*, Construction Press, London.
Neilsen, L.F. (1970), "Kriechen und Relaxation des Betons", *Beton- und Stahlbetonbau,* **65**, 272-275.
Rusch, H., Jungwirth, D. and Hilsdorf, H. (1973), "Kritische Sichtung der Einflusse von Kriechen und Schwinden des Betons auf das Verhalten der Tragwerke", *Beton- und Stahlbetonbau,* **68**(3), 49-60, No. 4, 76-86; No. 5, 152-158.
Schade, D. (1977), "Alterungsbeiwerte fur das Kriechen von Beton nach den Spannbeton-richtlinien", *Beton- und Stahl- betonbau,* **72**(5), 113-117.
Sun, S.C-H. (1996), "Nonlinear analysis and design of concrete framed structures", PhD Thesis, The

University of New South Wales, Sydney, Australia.
Trost, H. (1967), "Auswirkungen des Superpositionsprinzips auf Kriech- und Relaxations-Probleme bei Beton und Spannbeton", *Beton- und Stahlbetonbau,* **62**, No. 10, 230-238; No. 11, 261-269.
Warner, R.F., Rangan, B.V. and Hall, A.S. (1989), *Reinforced Concrete*, 3rd edn, Longman Cheshire, Melbourne.
Whitney, C.S. (1932), "Plastic theory of reinforced concrete design", *Transactions, ASCE,* **107**, 251-326.